

# A long-term assessment of fire regimes in a Brazilian ecotone between seasonally dry tropical forests and savannah



Daihana S. Argibay\*, Javier Sparacino, Giovana M. Espindola

PRODEMA, Federal University of Piauí, 64049-538 Teresina, Brazil

## ARTICLE INFO

**Keywords:**  
Seasonality  
Fire recurrence  
Caatinga  
Cerrado  
Precipitation

## ABSTRACT

Fire is a recurrent phenomenon in semiarid seasonal ecosystems. The study of the relationship between fire and climate could provide new approaches for understanding fire dynamics in semiarid regions, which could be useful for strategically managing the loss and recovery of natural resources under threat. Here, we evaluated the patterns of fires occurrence in a semiarid Caatinga-Cerrado ecotone in the Northeast Region of Brazil by characterizing their spatiotemporal dynamics associated with climatic conditions. Using a temporal series of 306 Landsat images, we mapped a burned area database at a fine spatial resolution (30 m) from 1999 to 2017 in the Capivara-Confusões Mosaic of protected areas and their surroundings. Fire seasonality was analyzed through climatic seasons, distinguishing between the rainy season (RS), early dry season (EDS), middle dry season (MDS) and late dry season (LDS), by analysis of the daily precipitation of ground-based stations in the area. We created yearly, seasonal and recurrence maps of burned areas to assess fire regimes. The results showed that the 48% of the area was burned during the 19-year long period considered. Serra das Confusões National Park (SCoNP) had 302,644 ha burned, Serra da Capivara National Park (SCaNP) had 2056 ha burned and the ecological corridor had 215,718 ha burned. Most of the burned area was registered during the MDS (36% of the study area), there was almost no burned area in the EDS ( $< 0.01\%$ ), while the LDS (7%) and the RS (4%) had similar dimensions burned. The years that burned the most (2001, 2007, 2010, 2012, 2015) were followed by years with considerably less burned area. We identified a multiple-year process, consisting of a climatological year with above-average precipitation and consequent low burned area, followed by a climatological year with below-average precipitation and resulting in large extensions of burned area (periods: 1999–2001, 2008–2010, 2010–2012). Fire recurrence reached a maximum value of ten, with 47% of the area burned presenting some degree of recurrence. SCaNP presented no fire recurrence, while SCoNP had a maximum recurrence parameter of four. Areas with moderate fire recurrence were near roads, settlements or cities. Some recurrently burned areas presented similar shapes, which were associated with topography limiting the spread of the fires. The patterns that we described here constitute the first step toward understanding the fire regimes of the region to establish directions for improving management strategies and orienting policies in the area.

## 1. Introduction

Fires alter the structure and composition of vegetation around the world, regulating the distribution of ecosystems (Bond et al., 2004). At the same time, vegetation is one of the key drivers in fire activity, regarding its productivity (biomass as fuel), flammability (chemical composition and structure), availability to burn (moisture/dryness) and phenology (deciduous, semideciduous or evergreen) (Archibald et al., 2018). Together with vegetation and fuel variation, climate, weather during fire, and ignition rates determine fire activity (Bradstock, 2010).

Fire regimes can be described as a particular combination of characteristics, such as frequency, intensity, severity, seasonality, size, type,

extent and spatial pattern of fire occurrence (Bond and Keeley, 2005). Fire regimes have been modeling the Earth processes for hundreds of millions of years, long before anthropogenic burnings (Scott, 2000). In spite of that, fire regimes are altered by human activities that play a complex role, influencing the number and timing of ignitions, suppressing fires, affecting the fuel amount and vegetation connectivity, and indirectly, altering climate (Archibald et al., 2013; Bowman et al., 2009; 2011; Flannigan et al., 2009; Mayr et al., 2018).

Worldwide, the spatial variability of fire regimes has been explained, in part, by rainfall seasonality and interannual variability, effective rainfall, the presence of long-term droughts and dry season length (Archibald et al., 2013; Argañaraz et al., 2015; Bradstock, 2010).

\* Corresponding author.

E-mail addresses: [archibayds@gmail.com](mailto:archibayds@gmail.com) (D.S. Argibay), [giovanamira@ufpi.edu.br](mailto:giovanamira@ufpi.edu.br) (G.M. Espindola).

<https://doi.org/10.1016/j.ecolind.2020.106151>

Received 18 February 2019; Received in revised form 18 January 2020; Accepted 28 January 2020

Available online 12 February 2020

1470-160X/ © 2020 Elsevier Ltd. All rights reserved.

These climatic variables are related to the annual probability of fire occurrence and the productivity that determines the fuel load (Archibald et al., 2009, 2013). Fire regimes are mostly associated with current vegetation and climate, but the complex interactions among fire, climate, vegetation and human activities difficult the capacity to predict fire emergence (Archibald et al., 2018).

Several authors have analyzed bioclimatic and anthropic variables that influence or alter fire regimes (e.g., Argañaraz et al., 2018; Mayr et al., 2018; Moreno et al., 2014; Nogueira et al., 2017a; Pourtaghi et al., 2016). On the one hand, annual precipitation and its distribution (Chen et al., 2017), as well as hot and dry days after a period of abundant rains (Archibald et al., 2009; Bradstock, 2010) could be mentioned between the climatic influences of the fire regimes. On the other, the main anthropic factors that drive fire occurrence worldwide are distance to roads, land use changes and the employment of fire for agricultural practices (Pourtaghi et al., 2016). Furthermore, the continuity of the fuel bed determines the spread of fire and can be confined not only by topography (natural) but also by roads or croplands that fragment the landscape (human) (Archibald et al., 2009).

In turn, seasonality, together with rainfall concentration, periods of pronounced water shortage, and fires are the main characteristics of semiarid environments (Archibald et al., 2013; Kousky and Chug, 1978; Murphy et al., 2013, Reddy, 1983). Semiarid ecosystems in the Neotropics encompass areas of savannah and seasonally dry tropical forest, in particular, Cerrado and Caatinga in central and northeastern Brazil, respectively (Collevatti et al., 2013).

The Cerrado is a savannah type ecosystem with a continuous herbaceous layer and its vegetation ranges from grasslands to open or closed shrublands and woodlands (Eiten, 1972, Coutinho, 1982). It has two well established seasons, with rainfall concentrated in a rainy season that lasts from six to seven months and the overall amount of rains is between 750 and 2000 mm/year (Eiten, 1972, Lehmann et al., 2011). The Caatinga is drier than the Cerrado, with several dry months and irregular rainfall concentrated in a short rainy season (generally three months). The annual rainfall of the Caatinga is mostly lower than 750 mm, but it can reach 1000 mm or be lower than 500 mm in some regions (Reddy, 1983; Prado, 2003). The Caatinga vegetation is discontinuous, ranging from deciduous low shrubs to small patches of tall dry forests well adapted to water shortage (Prado, 2003). While natural fires due to lightning have been recorded during the rainy season in the Cerrado (Ramos-Neto and Pivello, 2000), most fires are currently anthropic (Pivello, 2011) in both ecosystems. There may be differences in fire regimes between these two ecosystems, especially due to the rainfall gradient. In the drier Caatinga, fires might be limited by fuel availability and in the wetter Cerrado, fires might be limited by fuel moisture (van der Werf et al., 2008).

In addition to the regular seasonality, the variations of precipitation and the presence of droughts in semiarid environments are frequently related to specific climatic anomalies, such as the El Niño Southern Oscillation (ENSO) (Liu and Juárez, 2001). Droughts are characterized by the delayed arrival of rains or the anticipated end of rainy seasons with precipitation values below the annual mean (Ramos, 1975; Sampaio et al., 2005). These precipitation anomalies and redistribution, when caused by ENSO episodes, alter fire activity; although, the activity is altered with a time delay because anomalous precipitation occurs during the rainy season and the fire activity occurs mainly in the dry season (Chen et al., 2017). On one hand, long periods of drought in the Caatinga reduce biodiversity and increase tree mortality (Sampaio et al., 1993; Liu et al., 2013), which indirectly can cause an increase in fire severity. On the other hand, droughts limit primary production during the rainy season, decreasing the fuel resources available to burn (Nogueira et al., 2017a).

In this context, mapping fire regimes is useful for evaluating ecological conditions, providing a deeper understanding of how spatial and temporal patterns and processes (such as climate, topography, fuel availability and vegetation dynamics and structure) influence fire

dynamics (Morgan et al., 2001). Maps of fire regimes provide appropriate information for understanding and evaluating the ecosystem changes, for characterizing fire risks, for fire management and for helping policymaker decisions.

For studying fire regimes is useful to combine the fire occurrence in association with seasonality (e.g., Alves and Pérez-Cabello, 2017). This information can be obtained through the application of satellite imagery in combination with ground-based rainfall observations, due to the continuous monitoring of land surface and climate. Remote sensing products have been used to map burned areas as the first step to characterizing fire dynamics, taking advantage of the particular spectral response of burned vegetation (Meng and Zhao, 2017; Mouillot et al., 2014; Key and Benson, 2006). After vegetation is burned, broad spectral changes occur that are associated with the combined effects of the removal of vegetation, increased soil exposure, the presence of ashes or charred vegetation and changes in the soil moisture (Lentile et al., 2006). Moreover, long time series data from sensors aboard Landsat satellites of fine spatial resolution were used to describe fire regimes for protected areas in the Brazilian Cerrado (Alvarado et al., 2017; Daldegan et al., 2014; Lemes et al., 2014; Melchiori et al., 2014). In contrast, no long-term study of fire has been conducted in the Caatinga regions. However, Moderate Resolution Imaging Spectroradiometer (MODIS) series, which offers daily information from 2000 to the present with lower spatial resolution, has been used for mapping burned areas at global, regional and local scales, that included some Caatinga regions (Chuvieco et al., 2016; Nogueira et al., 2017a,b, among others).

Despite the existence of some studies of fire dynamics in semiarid environments, little is known about fires in Caatinga and its transition with the Cerrado ecosystem. Thus, information on the relative importance of several environmental factors affecting burned areas in this region is currently lacking, particularly for protected areas. In this work, we aim to create a burned area database of fine spatial resolution and to explore how climate influences fire regimes in a Mosaic of protected areas located in the Cerrado-Caatinga ecotone (Northeast Brazil). We used a combination of Landsat series for burned area delimitation and ground-based rainfall observations for climate season classification. We analyzed fire incidence from 1999 to 2017 to answer the following questions: i) how does fire occurrence vary in time and in space over these 19 years across the Capivara-Confusões Mosaic? ii) how do seasonality and precipitation anomalies influence fire patterns? iii) how is fire recurrence spatially distributed?

## 2. Materials and methods

### 2.1. Study area

The present study was conducted in the Capivara-Confusões Mosaic (CCM, Fig. 1) located in the southwestern section of Piauí state in the Northeastern Region of Brazil. The CCM is composed of Serra da Capivara (SCaNP) and Serra das Confusões (SCoNP) National Parks and the ecological corridor between them. Our study area includes approximately 84% of each National Park and the whole corridor and it was defined including a surrounding area of 25 km radius around the CCM and cropped to fit the limits of the state of Piauí at the south and the Landsat scene path/row 219/66 to the east and southwest. The total area is 2,213,643 ha, placed between 8°9′–9°25′ S and 44°13′–42°22′ W (Fig. 1).

The SCaNP was created in 1979 and covers a surface area of 134,973 ha. The park was declared as a World Heritage site by the United Nations Educational, Scientific and Cultural Organization (UNESCO) in 1991 due to its archaeological legacy. It presents evidence and artifacts related to the origins of human settlement in the continent, including the largest concentration of rock paintings and archaeological sites in the Americas (Lahaye et al., 2013). The whole park is crossed by a web of dirt roads that give access to the different archaeological sites

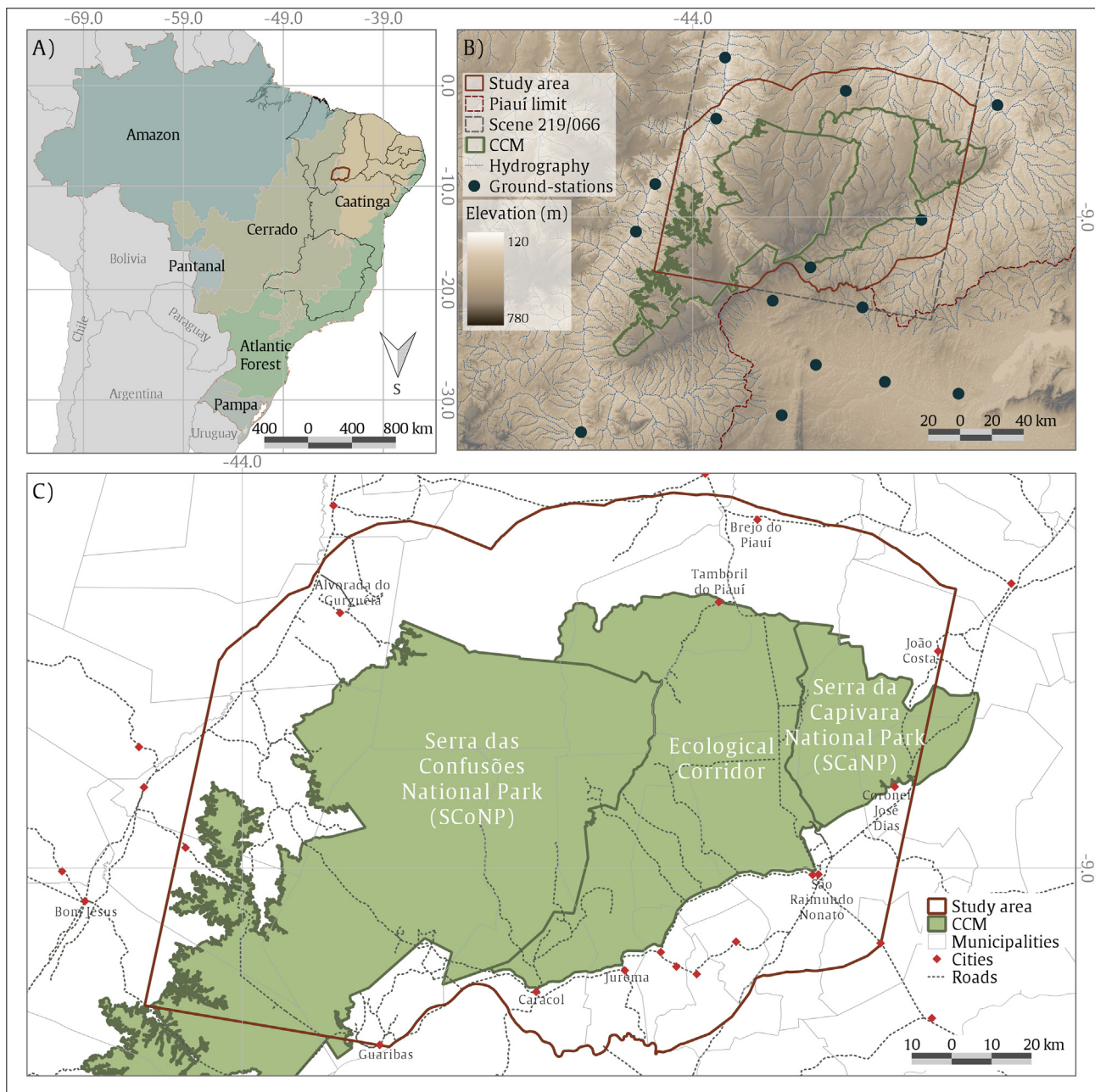


**Fig. 1.** Map of the study area: (A) location of the study area in the context of Brazil representing the different fitophysioognomies recognized by the Brazilian Ministry of the Environment (MMA, 2017); (B) altimetric ranges extracted from the Shuttle Radar Topography Mission (SRTM) digital elevation model (Jarvis et al., 2008; U.S.G.S., 2006), hydrologic courses (ANA, 2017) and location of the meteorological stations from ANA and INMET; and (C) context of the CCM (Capivara-Confusões Mosaic) in the state of Piauí municipalities and roads (IBGE, 2017).

for visitation and may act as firebreaks (Olmos and Albano, 2012).

The SCoNP was created in 1998 and currently covers 834,129 ha. Even though hunting is prohibited, the park presents some hunting problems due to its dimensions and lack of monitoring staff. Moreover, it is crossed by dirt roads that link the cities from the southeast to the northwest, and it has some villages in its boundaries. Both parks are managed by the Chico Mendes Institute for Biodiversity Conservation, which belongs to the Brazilian Ministry of Environment (ICMBio and MMA – acronyms in Portuguese, respectively).

The CCM was created through a federal decree in 2005 to integrate the management of the two National Parks, their buffer areas and the ecological corridor between them. The principal purpose for its creation was the conservation and sustainable use of natural resources to provide effective preservation of biodiversity. Nevertheless, the corridor is

crossed by some paved roads, and several settlements exist with extensive agriculture and cattle raising. Fire is commonly used as a management practice for land preparation for cultivation.

The CCM is located between the two largest geological formations in Northeast Brazil: the Parnaíba River sediment basin, which is a Silurian-Devonian sandstone formation, and the peripheral depression of the São Francisco River, with small Precambrian limestone formations (Lemos and Rodal, 2002). The main sandstone plateau, locally known as *chapada* (Fontugne et al., 2013), reaches 700 m and is bounded by 50–200 m cliffs and dissected by valleys and canyons (Silveira et al., 2010). The limestone formations emerge as island mountains between the *chapada* and are deeply eroded with many cavities, rock shelters and caves (Fontugne et al., 2013). Soils from the *chapadas* are mainly yellow-red latosols, while in the valleys and canyons have

predominately white sand (Olmos, 1992). There are no perennial watercourses inside any of the parks, but there are perennial natural sources in SCoNP and some intermittent rivers during the rainy season; artificial reservoirs are also maintained in SCoNP and filled in the dry season to supply fauna as a management practice (Olmos and Albano, 2012).

The study area is characterized by a semiarid climate with a long dry period and a short rainy season. The 68% of the annual precipitation is concentrated between December and March (Sparacino et al., unpublished manuscript) and the vegetation is adapted to the annual water shortage (Reddy, 1983). The eastern region of the study area presents a mosaic of different assemblages of thorny, xerophyte and/or deciduous Caatinga vegetation (Empeiraire, 1989; Olmos, 1992; Silveira et al., 2010) with a transition to the southwest presenting a Cerrado savannah vegetation characterized by a ground layer of grasses, shrubs and trees (Miranda et al., 2009). The vegetation within the *chapadas* has a shrubby-arboreal structure with low height (6–10 m); the canyons, which are wetter, present semideciduous forest enclaves with taller vegetation (up to 30 m). The cliffs present an arboreal structure with individuals reaching more than 15 m height and separate the *chapadas* from the plains that present medium-height forest (5–10 m) (Empeiraire, 1989; Moura, 2005a). The woody vegetation starts to lose its leaves in May, producing abundant leaf litter, and by August, most of the trees are leafless (Moura, 2005a). There is also a seasonal herbaceous component that dies during the dry season (Lemos and Rodal, 2002). In the Caatinga-predominant region, the herbaceous component is discontinuous, so foliage, litter and fine woody debris are the major fuels for combustion and fire spread, with fires regularly reaching the canopies (Kauffman et al., 1993), while in the Cerrado-predominant region, the fuel consumed is from the continuous herbaceous layer (forbs and grasses) (Miranda et al., 2009). Studies of Caatinga woody vegetation regeneration after wildfires are still lacking, nevertheless, was reported that some species resprout after slash-and-burn practices (Sampaio et al., 1993, 1998). In the Cerrado ecosystem, the woody component resprouts after fire and the herbaceous component recovers rapidly few days after the fire (Miranda et al., 2009).

## 2.2. Data acquisition and processing

The steps followed during the course of this work are graphically presented in Fig. 2.

### 2.2.1. Satellite imagery and burned area database

For the delimitation of the burned areas, we worked with a temporal series of Landsat 5 Thematic Mapper (TM), Landsat 7 Enhanced

Thematic Mapper Plus (ETM+), and Landsat 8 Operational Land Imager (OLI) sensors with a spatial resolution of 30 m (Table 1). A total of 306 Landsat images (path/row 219/66) were used covering the time period between 1999 and 2017 (Fig. 3), excluding those completely covered by clouds. The vast majority of fires occurred during the dry season when it was mainly cloudless, allowing the view of land surface for fire scar identification (Feeley et al., 2005; Sano et al., 2007). The burned areas were identified by visual interpretation, and when a scar was partially covered by clouds, obstructing its correct spatial delimitation, its date was registered but later images were used for the delimitation, as the scars remain visible in the next consecutive images during the dry and wet seasons (Alvarado et al., 2017). The temporal resolution of the Landsat satellites is 16 days, but we were able to reduce this to 8 days for some periods using the images from satellites that are in orbit simultaneously (Fig. 3). Thus, we analyzed an average of 16 images per year (minimum 7 and maximum 22), depending on cloud-free image availability. The ETM+ sensor had a failure on its Scan Line Corrector mirror in 2003, so images were matched with each other and with TM and OLI sensors to fill the gaps using a simple overlay for image interpretation purposes.

We used LEDAPS data (Landsat Ecosystem Disturbance Adaptive Processing System, Masek et al., 2006) for Landsat 5 and 7 and LaSRC data (Landsat 8 Surface Reflectance Code, Vermote et al., 2016) for Landsat 8 products, both from Collection-1, which are radiometrically calibrated and orthorectified using ground points and digital elevation model data to correct for relief displacement, and the on-demand Level-2 products interface, which corrects the images for atmospheric effects at the surface reflectance level (USGS, 2018). All images were ordered and downloaded from the USGS (U. S. Geological Survey web page).

For the identification of burned areas, we generated RGB false color composites for each image using short wave infrared (SWIR), near-infrared (NIR) and green wavelengths (Table 2). In this way, fire scars were visualized in magenta hues surrounded by a green matrix, with white clouds and black cloud shadows. The NIR and SWIR bands are often used to study biomass consumption from fire, such as the severity of the burned areas, as the NIR naturally reacts positively to the foliar area and productivity and the SWIR reacts positively to the drought and no vegetated surfaces (Key and Benson, 2006; Keeley, 2009). Therefore, the combination of the high reflectance NIR with the low reflectance SWIR allows us to distinguish between burned and unburned vegetation (Meng and Zhao, 2017).

Each fire scar was visually identified, first at a 1:180,000 scale, and manually vectorized using a 1:24,000 scale (Key and Benson, 2006) to build a spatial-time fire scar polygons database. This exhaustive method had previously been used by some authors for the identification of burned areas (Alvarado et al., 2017; Alves and Pérez-Cabello, 2017; Eidenshink et al., 2007), for some government agencies (Portugal: ICNF, 2018; United States, MTBS: Eidenshink et al., 2007), and to validate the accuracy of automatic detection of burned area algorithms (Bastarrika et al., 2014; Cardozo et al., 2014; Libonati et al., 2014; Melchiori et al., 2014) to estimate the omission/commission errors. This technique was preferred over the different products now available for burned areas detection (MODIS: MCD45A1 and MCD64A1, GFED4 and GFD4s; INPE: AQM: Libonati et al., 2015; BAMS: Bastarrika et al., 2011, 2014; ESA Fire\_cci project: Chuvieco et al., 2016) because none of them was exclusively designed for this kind of ecotone among savannah and dry forest environments. We then assigned to each delimited scar polygon the date of the image when it first appeared. The fires that were active during the satellite data acquisition (image) are thus registered by parts, each having a different date. For this reason, we limited our analysis to the total burned area by year and season and avoided assessing fire-size classifications.

For validation purposes, we made two field campaigns to the parks in May and June 2018, and we visited three fire scars of different ages in each park. These fires occurred in 2017, 2015 and 2010/2011, so we were able to recognize the differences in vegetation damage and

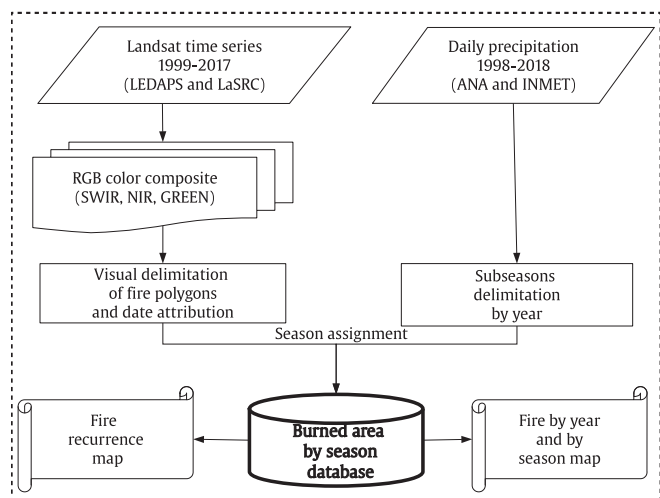
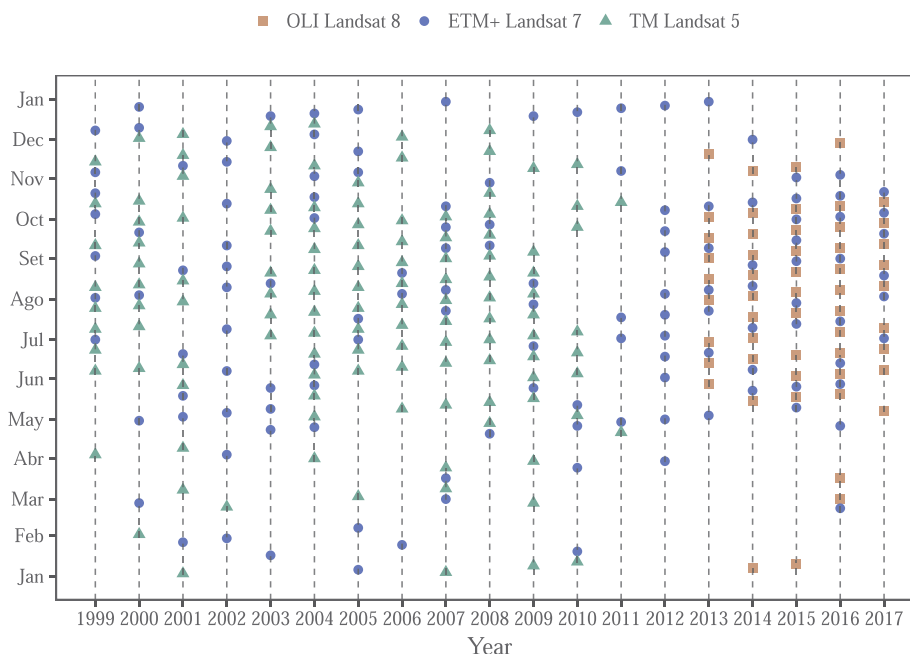


Fig. 2. Flow chart of methodological procedures.

**Table 1**  
Information about satellites and respective sensors used as sources for image analysis.

	Satellite	Sensor	Spatial resolution	Temporal resolution	Availability
LT5	Landsat 5	TM	30 m	16 days	March 1984–November 2011
LE7	Landsat 7	ETM+	30 m	16 days	April 1999–present
LC8	Landsat 8	OLI	30 m	16 days	February 2013–present



**Fig. 3.** Representation of the database used for scar delimitation. Date, satellite and sensor information of the images are described.

recovery over time. The fire scars were delimited previously by visual interpretation of remote sensing data, and field verification was made of some points of the scar limits. We also checked some nonburned islands in a 2017 SCoNP fire scar to prove their existence. See [Appendix A](#) for more details, including exemplary imagery comparing *in situ* burning with Landsat images and digitalized burned areas ([Fig. A1](#)).

The fire scar polygons database was used to assess the spatial and temporal patterns of burned areas. We worked with polygons larger than 5 ha. The spatial dynamics were analyzed for the complete study area and separately for each park and the ecological corridor to be best suited for management purposes. Since external fires can affect the boundaries of the parks, we analyzed their burned area using a 2 km buffer from their borders. The temporal dynamics of burned area were analyzed by month, year and season.

**2.2.2. Climatic data, seasonal classification and fire recurrence map**

Daily precipitation was obtained from the Brazilian National Water Agency and the Brazilian National Institute of Meteorology (ANA and INMET – acronyms in Portuguese, respectively). Data from 15 meteorological stations ([Fig. 1B](#)) were averaged for the best characterization of the study area and to address incomplete data sets from individual stations. The details of the climatic characterization of the study area can be found in [Sparacino et al. \(unpublished manuscript\)](#);

here, we only present a summary.

For the rainy (RS) and dry seasons (DS) characterization of each of the nineteen years (1999–2017), we organized data in climatological years beginning on July 1 (the driest month) and ending on June 30 of the following year. The date of the onset and the end of the RS of each climatological year was determined following [Liebmann et al. \(2007\)](#) by analyzing the anomalous accumulation, a quantity constructed to identify the beginning and end of precipitations from accumulated daily anomalies. Each dry season (DS) is the time period from the end of one RS until the beginning of the next RS (is, then, associated to a calendar year, from January 1 to December 31 of the same year). Thereafter, each DS was subdivided following [Alves and Pérez-Cabello \(2017\)](#), considering the longest period of consecutive days with daily precipitations below 5 mm as the middle dry season (MDS), representing the driest period of the DS. The remaining days at the beginning and at the end of the DS represent the two transition periods from and to the RS and are identified as the early dry season (EDS) and the late dry season (LDS), respectively.

We classified fires into seasons in line with their date of occurrence, and each fire scar polygon was then associated with one climatic season. The temporal resolution and, thus, the accuracy of this season classification of fires depends on satellite image availability (minimum time between images was 8 days). Since fire date attribution

**Table 2**  
Description of spectral information of the different bands and sensors used to generate the RGB color composite for scar delimitation.

Sensor/Band	GREEN	NIR	SWIR2
TM/5	Band 2 0.52–0.60 μm	Band 4 0.76–0.90 μm	Band 7 2.08–2.35 μm
ETM+/7	Band 2 0.52–0.60 μm	Band 4 0.77–0.90 μm	Band 7 2.09–2.35 μm
OLI/8	Band 3 0.533–0.590 μm	Band 5 0.851–0.879 μm	Band 7 2.107–2.294 μm

corresponded to its first visualization, its genuine date of occurrence could be any one day between the day after the previously available image and the day of the image when the scar was first seen. If the date of the previously available image corresponded to the same season classification as the one in which the fire was determined, the season classification was unambiguously determined, which was the case for 84% of the scars. On the other hand, 16% of fires occurred near a season transition, i.e., the previously available image belonged to a different season; thus, its corresponding season could not be determined unambiguously. For those cases, the season that corresponded to the date in which the scar was observed for the first time was attributed and was distributed as follows: 0.02% associated with the EDS, 0.45% with the MDS, 8.74% with the LDS, and 7.10% with the RS.

Following the fire seasonal classification, we developed maps of the spatial distribution of the scars across the climatic seasons over the years. These maps were used to better understand the patterns, seasonality and conditions of each fire, as well as their proximities to the parks. Annual and monthly patterns of precipitation were analyzed and linear regressions and correlations were tested in order to describe statistical relations between burned area against precipitation amounts and seasons length.

For the compilation of the recurrence map, we first constructed 19 annual maps and converted them into 19 binary rasters ( $I$  = burned,  $O$  = not burned) of 30 m resolution and then summed the values of the input maps. In this way, the recurrence parameter associated with each pixel was obtained. For data manipulation, we used Quantum-GIS 2.18.14 'Las Palmas' (QGIS Development Team, 2018), and R 3.5.1 (R Core Team, 2018), with packages 'rgdal' (Bivand et al., 2015) and 'raster' (Hijmans, 2017).

### 3. Results and discussion

#### 3.1. Yearly patterns of burned area

From 1999 to 2017, the total burned area in the Capivara-Confusões Mosaic (CCM) and its surroundings was 1,056,764 ha, distributed in 4824 fire scars, representing an equivalent of 48% of the total study area (Table 3). From that, 597,353 ha burned at least once (27% of the study area), and this extension burn had a crucial significance concerning these protected areas. A slight reduction in the total burned area was registered after the creation of an environmental protected area in a Cerrado region of central Brazil (Alvarado et al., 2017), but we could not analyze the CCM efficiency because the period under study was after the parks creation.

The annual burned area was very dissimilar for the 19 years considered. Between the years with the least and most burned areas, there were two orders of magnitude differences. The years 2015 and 2010 had the most burned area, with 188,452 and 174,553 ha, respectively, followed by 2012 (107,197 ha), 2007 (106,452 ha) and 2001 (84,275 ha) (Table 3 and Fig. 4). In contrast, the years 2006, 2003 and 2014 registered the three lowest annual burned areas with 9575, 13,893 and 13,156 ha, respectively.

The analysis of annual burned area demonstrated that the years with the largest burned extensions were always followed by a year with considerably less burned area (Fig. 4). This could mean that from one year to the next, there was not enough biomass accumulated to act as fuel to cause fires of large dimensions because it was already burned. According to Alves and Pérez-Cabello (2017), the burned area in a year controls and delimits the area that will burn the next year, probably because the fuel loads are limited by the propagation of the fire from the previous year. That trend can be observed by comparing the five most burned years with the corresponding following year (2001–2002, 2007–2008, 2010–2011, 2012–2013, and 2015–2016, Fig. 4).

Furthermore, it is noticeable that those years with large extensions of burned area occurred with one or two years in between, similar to some Cerrado environments (Alvarado et al., 2017; Alves and Pérez-

Cabello, 2017). This short fire return interval can be explained by the intrinsic characteristics of tropical ecosystems, with high rates of recovery and net production (Field, 1998), meaning the fast accumulation of fire-prone biomass as fuels. Over the seasonally dry tropical forest, biomass production occurs during the RS and increases with the amount of precipitation, overwhelmingly after the DS (Martínez-Ramos et al., 2018). We assume that the biomass produced during a RS and not consumed by a fire in the immediate DS would be accumulated together with the new biomass generated in the following RS and would become fuel with high probability to burn because of its low moisture content.

Precipitation indirectly controls fire activity by the biomass production and, thus, by the availability of fuels (Mayr et al., 2018). We could not find a relationship between the accumulated precipitation during the previous RS and the annual burned area ( $p = 0.380$ ,  $r = -0.214$ ,  $R^2 = 0.046$ ). This suggests that the amount of biomass produced (directly related to the amount of precipitation) in the previous RS is not the only parameter controlling the amount of burned area during the fire season, especially because precipitation will determine the fuel moisture that limits the extension of fires (Alvarado et al., 2017; Argañaraz et al., 2018) and because in arid savannas fire activity is actually associated with the accumulated precipitation of up to two RS (Alvarado et al., 2019). As an example, this was the case in 2012, which had large extensions of burned area despite the presumably low biomass productivity during the growing season. In fact, the precipitation of the 2011–2012 RS was the lowest in the period (433 mm, Sparacino et al., unpublished manuscript) as a result of a drought in Northeast Brazil, while the amount of burned area in 2012 was the third largest. The 2011–2012 drought occurred exceptionally during La Niña, which is normally associated with enhanced precipitation in the region; reduced precipitation is usually associated with El Niño (Marengo et al., 2017; Rodrigues and McPhaden, 2014).

A multiple-year process could explain the large extensions that burned in some of the years. That process consists of the combination of a climatological year with above-average precipitation followed by a climatological year with below-average precipitation. In this way, a large amount of biomass is produced in the first year with above-average precipitation but does not burn, then accumulates and is particularly dry during the second year with below-average precipitation, leading to large burned areas. This pattern can be identified in association with three of the five years with the most burned area: 2001, 2010 and 2012 (Fig. 4). As an example, the annual precipitation in climatological year 2010–2011 was 854 mm, above the average for the area (749 mm is the normal annual precipitation, average data from 35 years, 1983 to 2018, Sparacino et al., unpublished manuscript), and the extension burned in 2011 was 19,995 ha. During the next climatological year, 2011–2012, precipitation was only 433 mm, and large extensions were burned during the year 2012 (107,197 ha). The same situation can be identified leading to the large burned extensions in 2001 (84,275 ha): a large amount of biomass was presumably produced during the above-average climatological year 1999–2000 (945 mm), accumulated (only 28,403 ha burned in 2000) and was presumably dry after the poor rainfalls of the climatological year 2000–2001 (671 mm). The pattern seems to also remain in the above-average 2008–2009 (866 mm) with few burned areas in 2009 (17,537 ha), followed by the below-average 2009–2010 (723 mm), leading to the large burned areas during 2010 (174,553 ha).

The other two years among those that had the largest burned areas are 2007 and 2015. On one hand, the large extensions burned in 2007 (106,452 ha) occurred after two climatological years with below-average precipitation, 2005–2006 (598 mm) and 2006–2007 (575 mm), but that were preceded by three climatological years with above-average precipitation: 2002–2003 (777 mm), 2003–2004 (888 mm) and 2004–2005 (827 mm). Thus, the processes leading to large burned areas can also be more complex than the multiple-year process that we suggest. On the other hand, from 2012 to 2016, Northeast Brazil suffered a long-term drought, with four consecutive climatological years

**Table 3**

Extension in hectares (ha) of annual burned areas separated by climatic season and categorized by SCaNP, SCoNP and ecological corridor. Annual burned extensions of the complete study area are also presented (CCM and surroundings), including the surroundings that do not belong to the parks or to the ecological corridor. The total burned area from 1999 to 2017 is presented both as an extension in hectares (ha) and as a percentage of the area of each category (SCaNP: 143,049 ha, SCoNP: 813,038 ha, ecological corridor: 397,706 ha, CCM and surroundings: 2,213,643 ha).

Year	Cativara-Confusões Mosaic (CCM)										CCM and surroundings									
	SCaNP			SCoNP			Ecological Corridor			DS			RS			Total				
	DS		RS	Total	DS		RS	Total	DS		RS	Total	DS		RS	Total				
	E	M	L	E	M	L	E	M	L	E	M	L	E	M	L					
1999	-	509	-	-	509	-	13,501	-	247	13,748	-	7184	-	467	7651	-	50,251	-	944	51,195
2000	-	15	-	40	55	-	2413	-	388	2801	-	5300	-	859	6159	-	24,635	-	3768	28,403
2001	-	309	-	164	473	-	6797	12,175	597	19,569	-	510	5760	5607	11,877	-	19,293	54,332	10,649	84,275
2002	-	-	9	-	9	-	200	5933	-	6133	-	90	4873	-	4963	-	8431	30,449	-	38,880
2003	-	-	-	-	-	-	1725	623	-	2348	-	840	443	-	1283	-	7005	6887	-	13,893
2004	-	-	-	-	-	-	4385	2195	744	7324	-	769	2249	918	3936	-	26,861	13,938	2994	43,793
2005	-	-	95	-	95	-	201	10,655	427	11,283	-	618	4323	783	5724	-	4290	33,441	2038	39,769
2006	-	-	-	-	-	-	414	-	50	464	-	-	1717	496	2213	-	6040	-	3535	9575
2007	-	-	-	-	-	-	25,125	-	11,444	36,569	-	20,619	-	993	21,612	-	93,645	-	12,806	106,452
2008	-	-	-	-	-	-	11,211	-	208	11,419	-	4876	-	710	5586	-	21,319	-	1076	22,395
2009	-	8	-	-	8	-	65	-	667	732	-	347	-	2420	2767	-	2238	-	15,299	17,537
2010	-	381	-	-	381	-	52,547	-	5521	58,068	53	45,490	-	1721	47,264	53	162,909	-	11,591	174,553
2011	-	-	-	-	-	-	4722	-	3062	7784	-	390	-	1414	1804	-	14,421	-	5574	19,995
2012	-	-	-	-	-	-	9439	-	13,459	22,898	-	7091	-	-	7091	-	90,856	-	16,341	107,197
2013	-	-	-	-	-	-	1114	542	-	1656	-	2609	2766	-	5375	-	7583	10,027	-	17,610
2014	-	-	-	-	-	-	2173	3475	-	5648	-	1519	25	-	1544	-	8514	4642	-	13156
2015	-	187	-	-	187	-	79,503	-	-	79,503	-	56,695	-	-	56,695	-	188,452	-	-	188,452
2016	-	-	-	-	-	-	2346	3479	1947	7771	-	10,806	4817	1807	17,430	-	40,420	11,394	7212	59,026
2017	-	339	-	-	339	-	6926	-	-	6926	-	4744	-	-	4744	-	20,606	-	-	20,606
Burned area (ha)	0	1748	104	204	2056	0	224,807	39,076	38,761	302,644	53	172,216	25,255	18,194	215,718	53	797,771	165,112	93,828	1,056,764
%	-	1	0.1	0.1	1	-	28	5	5	37	0	44	7	5	56	0	36	7	4	48

SCaNP: Serra da Capivara National Park; SCoNP: Serra das Confusões National Park; DS: dry season; RS: rainy season; E: early dry season; M: middle dry season; L: late dry season.

with below-average precipitation, which was considered the most severe in recent decades. Some authors related the drought to La Niña (2011–2012) and El Niño (2015) ENSO events (Barbosa et al., 2019; Marengo et al., 2017; Rodrigues and McPhaden, 2014) that were described as fire drivers by Chen et al. (2017). Therefore, as severe droughts increase tree mortality in semiarid ecosystems (Liu et al., 2013), leading to more fire-prone fuels, the more recent large extension burned in 2015 is presumably related to extremely dry conditions. The reducing levels of annual precipitation and the increasing number of consecutive dry days in our study area (Sparacino et al., unpublished manuscript) can be associated with the fact that droughts are becoming more severe due to global warming (Dai, 2011). This is relevant

considering that droughts increase fire-related carbon emissions (Aragão et al., 2018) and will have as consequence a positive feedback in global warming.

### 3.2. Spatial and seasonal distribution of burned area

The burned area inside the CCM represents approximately half of the total burned area between 1999 and 2017, however, the CCM covers the 60% of the study area. So, if we consider separately the extensions occupied by the CCM (1,333,913 ha) and by the surroundings (879,730 ha), the incidence of fire inside the CCM is, in fact, smaller than outside (total burned area of the CCM and the

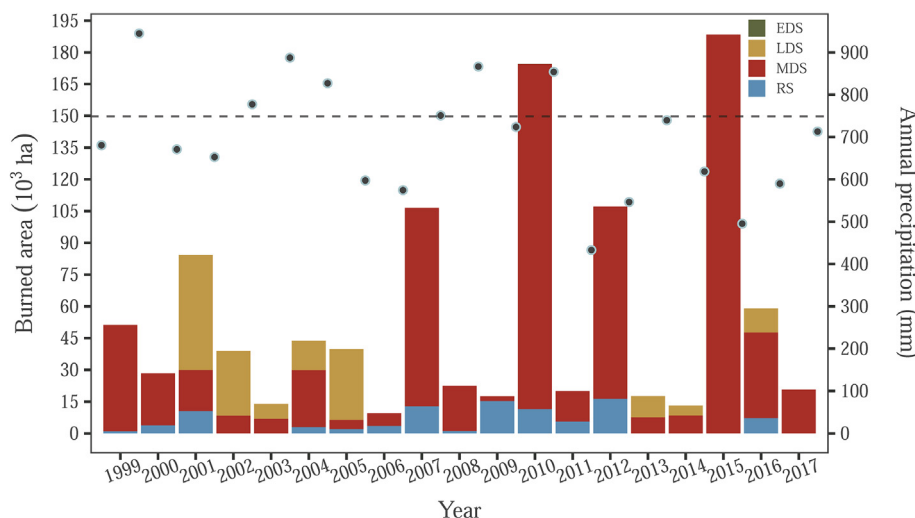


**Fig. 4.** Yearly distribution of burned area differed by season in the calendar year. The fires of the rainy seasons take place mostly during the beginning of the rainy season at the end of the calendar year (only 0.06% of the burned area takes place between January and May). Black points represent annual precipitation of each climatological year, from July 1 to June 30 of the next year (data from ANA and INMET). EDS: early dry season; MDS: middle dry season; LDS: late dry season; RS: rainy season. There was only one fire of 53 ha during EDS in 2010 and is not visible in the figure.

surroundings was equivalent to 37 and 65% of its respective extensions). Thus, protected lands appear to contribute to the reduction of fire occurrences in the region, even though, without achieving the “zero-fire” policy which was one of the main purposes for the creation of the protected areas in Brazil (Schmidt et al., 2018).

Furthermore, fire incidence is very dissimilar between each of the three parts of the mosaic. In the ecological corridor, fire affected an area equivalent to 56% of its total extension, while in the SCoNP it represented 37%, and in the SCanP, only 1% (Table 3). The proportion burned in the ecological corridor is closer to that of the surrounding CCM than those of the parks, and it seems that it is not achieving the purposes of its creation in an effective way. Additionally, there are contrasting realities among both parks, with almost not burned areas in SCanP compared to 37% of the areas affected in SCoNP, which can only partially be explained by its dimensions.

The SCoNP had a total of 302,644 ha burned (Table 3), with the largest fire scar of approximately 55,423 ha in 2015. This large-proportion fire grew with active fires from three different ignition points. The first detection of the scar was August 22, and it continued growing during nine images until November 02. Most of fires affecting the park started outside the boundaries and spread into the park. However, some scars were detected completely inside the limits of the SCoNP, evidencing practices that can cause ignitions there, such as the use of fire for cooking and warming in illegal hunting camps, for wild honey collection, or for intentional burning of land for cultivation, among others. Evidence of this kind of activity was found during the field campaigns made by the research team where we encountered hunters and found remains of campfires, a practice that was also described by Moura (2005b). In addition, the dirt roads that cross the park are poorly maintained, which makes access to combat fires difficult. During the field campaigns, we also noticed that on some roads, there are many trees crossing the roads, blocking the way and reducing the effect of the roads as firebreaks. However, the fire-exclusion policy in the protected areas of the Cerrado has been rethought in order to recover the natural fire regimes of the ecosystem by the application of prescribed burns (Batista et al., 2018; Durigan and Ratter, 2016; Schmidt et al., 2018). The implementation of an Integrated Fire Management (IFM) Program for the SCoNP should be considered, especially on its western region that is Cerrado-predominant.

The SCanP had 2056 ha burned, most of them during 1999, 2001, 2010 and 2017. The largest fire scar was 475 ha in 2017. The park has strict control at every entrance, and there are many more staff working in the field than in SCoNP for a smaller area (Oliveira and Bernard, 2017), which seems to be effective in preventing fires. In the ecological corridor, 215,718 ha were burned, with the two largest fires occurring in 2010 (15,692 ha) and in 2015 (14,070 ha). Ignitions were likely due to land preparation for cultivation, since fire is used to clear the material after cutting it, a practice known as “slash and burn”. When it is practiced near forest boundaries, it is possible that, depending on fuel availability, fuel moisture and weather, fire spreads out-of-control, affecting large extensions. As the SCanP is completely located in Caatinga, and the knowledge of fire in this ecosystem is very scarce, is difficult to implement an IFM, so more studies are needed to fill this gap, such as vegetation and soil resilience and recovery after fire. It is worth mentioning that ICMBio fire brigades consist of personnel employed yearly for six months during the DS in each park, but there is no specific fire brigade working in the corridor.

The seasonality of the entire time period under study can be seen in Fig. 5, where the RS, EDS, MDS and LDS are identified. It can be seen that dry periods (EDS, MDS, and LDS together) extend longer than the RS for most of the years. Additionally, the strong seasonality of the area is reflected by the fact that the two transition stages (EDS and LDS) between the driest and the wettest periods of the year are absent in several years. In fact, the years 2006, 2008, 2012 and 2015 presented neither EDS nor LDS, and the dry season consisted only of a very dry period (MDS). Also, some years presented only one transition stage;

2005 had no EDS, while 2007, 2009, 2010, 2011 and 2017 had no LDS.

The annual maps with the spatial distribution of fires classified by season can be seen in Fig. 6. These maps ensure the visual analysis of the size of the scars, their spatial distribution across the different parts of the CCM and surroundings, and especially the seasonal patterns of occurrence. Thus, it can be noted that the largest scars occurred mainly during the MDS, such as the largest scar in the western part of the SCoNP that occurred in 2015 and the two largest scars in the ecological corridor (2010 and 2015), as mentioned above. Other scars of vast extension occurred in the surroundings in 2007, 2010, 2012, 2015 and 2016 during the MDS. Likewise, most burned areas both in general and for each particular year occurred during the MDS (Table 3 and Fig. 4). Exceptions occurred in 2001, 2002, 2005 and 2013, which had the largest burned area during the LDS, and in 2009, which had the largest burned area during the RS. As expected, most of fires occurred in the MDS, the driest period of the year, and they might be caused by the low moisture content of the accumulated biomass. This was also reported for an enclave of savannah vegetation in the Brazilian Amazon (Alves and Pérez-Cabello, 2017).

The MDS lasted  $165 \pm 34$  (mean  $\pm$  standard deviation) days on average over the 19 years studied and extended much longer than the EDS ( $28 \pm 28$  days mean length) and the LDS ( $22 \pm 30$  days mean length) for most of the years. Exceptions were in the years 2002 and 2003, when the EDS, MDS and LDS had similar lengths. Since the MDS is the driest period of the year, longer MDS could be associated with a greater amount of burned areas; in fact, the 5 years with the higher burned area (2001, 2007, 2010, 2012 and 2015) had intermediate or long MDS (127, 224, 157, 219 and 195 days, respectively). However, a linear regression between the yearly burned area and MDS length presented no significant results ( $p = 0.225$ ,  $r = 0.292$ ,  $R^2 = 0.085$ ). Also, the lack of transition seasons cannot be directly associated with more burned areas, because between the years with only MDS, whereas 2012 and 2015 presented large burned areas, 2006 and 2008 did not.

There was almost no fire scar during the EDS, and only a small fire event (53 ha) took place in 2010 within the ecological corridor (Table 3 and Fig. 6). In addition to its short length, the attenuated levels of rain seem to be enough for the biomass to remain wet during this season, preventing fire occurrence. Hoffmann et al. (2012) also found that fires in the Cerrado during the EDS are rarely large because of the high humidity and the absence of a continuous grass layer in the forest areas. Here, it could also be explained by the absence of ignition events associated with the “slash and burn” practice during this season, as it is in the slash stage in which live vegetation is cut, and it is not burned until the end of the DS (Claval and de Freitas, 2007).

The LDS was the second season with the most burned area (165,112 ha) behind the MDS. It is reasonable that comparing the two transition stages, the LDS represented the most fire-prone, since the dryness accumulated during the previous season could not be counterbalanced by the precipitation that is just starting to fall. The RS, which is, of course, the wetter season, presented a total of 93,828 ha burned composed mainly of small scars, with the only exception being a scar larger than 10,000 ha in 2012 (Fig. 6). In this way, the RS was just slightly less fire-prone than the LDS (the percentages of the study area burned in each season were 4% and 7%, respectively; Table 3).

Analyzing monthly rainfall and fire patterns together, it can be noticed that fires detected in the RS occurred mostly in the beginning of the season, during November and December (Fig. 7), when the vegetation was presumably still dry (similar to the situation in the LDS). Furthermore, from January to May (RS and EDS), there were almost no detection of new fire scars (only 0.06% of the total burned area occurred during these months). Burned area monthly distribution shows that fires frequently started in June (during the MDS), and its occurrence extended until December (LDS and beginning of RS). September is the month when the rain starts, but at low rates, while from October to December, the rainfall increases progressively until it peaks in March, when it starts to decrease. Most fires took place between

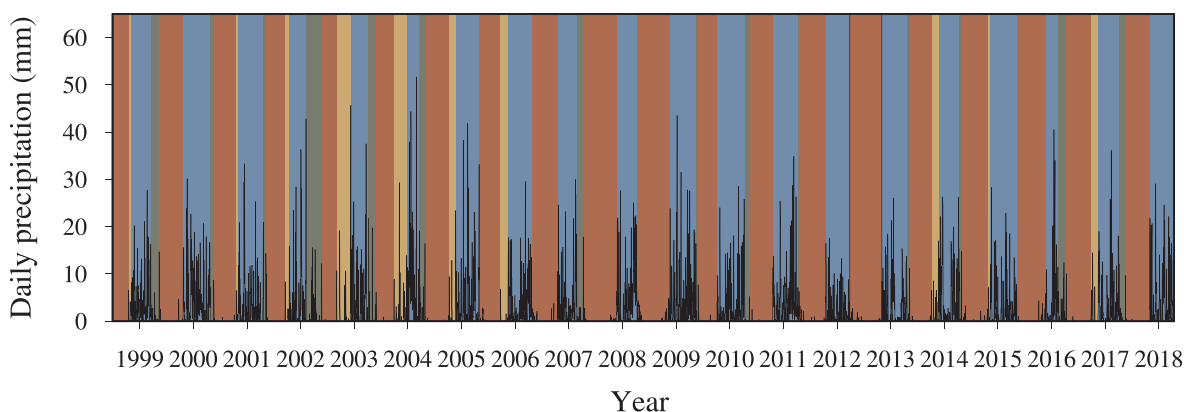


Fig. 5. Daily precipitation and season classification from 1999 to 2017. Early dry season (EDS) is colored in green; middle dry season (MDS) is colored in red; late dry season (LDS) is colored in yellow; rainy season (RS) is colored in blue. EDS, MDS and LDS together represent the whole dry season (DS). Daily precipitation is represented by the black curve based on ANA and INMET data (Sparacino et al., unpublished manuscript).

September and November, with a peak in October. Note that the driest months (June to August) were not the most burned. This suggests that the biomass produced during the RS needs several months after the end of rains to be dry enough to become fire-prone fuel to cause large fires (Fig. 7).

In the Cerrado, natural (lighting) fires are expected to occur mainly at dry-rainy season transitions (LDS) (Ramos-Neto and Pivello, 2000), while prescribed burns are executed during the rainy-dry season transitions (EDS). The former, burn the dry biomass and fire is extinguished naturally by the rains associated with thunderstorms. The latter, are designed to reduce the biomass able to burn in the DS, reducing fire intensity and severity. This way, the prescribed EDS fires applied in other Cerrado protected areas aim to create landscape mosaics with different fire histories to reduce the areas affected by LDS wildfires and decrease wildfire frequency in fire-sensitive vegetation (Schmidt et al., 2018). Fires found in the CCM are driven mainly by human activities, as most of them took place during the MDS, with timing associated to more severe, extensive and difficult to manage fires, affecting the conservation requirements of fire-vulnerable species. Hence, for maintaining the typical open and grassy physiognomies of the Cerrado, as well as fire-dependent species, relatively frequent fire is essential (Batista et al., 2018).

### 3.3. Fire recurrence map

A fire recurrence map is presented in Fig. 8, where the different colors represent the number of fires during the 19 years studied. For all the areas that burned at least once, 47% presented some degree of recurrence, ranging between two and ten. This means that an area that was burned had approximately half the chance to burn again along a 19-year interval and that the most frequently burned areas received a fire approximately every two years. However, the areas that burned more than six times represented only 0.1% of the total burned area. Fire recurrence could be associated with the high flammability of dead biomass and charcoal that resulted from previous fires and to the biomass fuels that resulted from the first regeneration stages.

The mapping of all scars together allows the description of general patterns of fire occurrence and recurrence and its association with different spatial parameters, which can be useful to build risk maps (Lemes et al., 2014). All scars that happened in the proximities and interior of SCanP burned only once and were mostly located near roads and settlements. The largest fires that took place in SCanP in 2017, in the southernmost corner, received strong media and societal repercussion and thus, in addition to fire brigades, volunteers, fire aircraft and firefighter brigades helped to control it, including staff from SCoNP.

In contrast, the interior area of SCoNP reached a recurrence parameter of four, and some areas of its proximities burned seven times

during the 19 years. Most of the fires that extended completely inside the boundaries of the park were in the proximities of the roads that cross it (Fig. 8) and could be interpreted as being human-caused. The dirt roads go mostly through natural courses that are mainly flat (locally named *baixões*) and confined by cliffs. Some fire scars burned areas with the exact shape of those *baixões*, so cliffs are acting as natural barriers that limit the extensions of fire. As an example, we can mention that for the scars that took place in the southern limit of SCoNP in 2008 and 2011, the shape of the scars appears to trace the cliff limits (this is more evident when compared with a topographic map, at a finer scale, not shown here).

Outside the western limits of SCoNP, which is closer to the Cerrado, several areas with moderate fire recurrence were recorded. The fires that occurred in 2004, 2007, 2012 and 2016 stopped when reaching the limits of the park (Fig. 6). This spatial confinement of fire could also be attributed to topography since the park is mainly located on a great plateau (locally named *chapada*). The abrupt limits due to slope differences presumably avoided the spread of fire into the park. Other fires that affected the SCoNP in the *chapada* were probably initiated inside the park (e.g., 2001, 2010, 2012, 2015).

Fires limited by topography were also found near the northernmost boundaries between the SCoNP and the ecological corridor, where similar areas were burned in 2007, 2010 and 2015. These *baixão* areas are frequently used as cultivation lands since they conserve humidity in an otherwise dry landscape. Therefore, the moderate fire recurrence found there may be associated with out-of-control fires used for land preparation. A similar situation was found within the southernmost boundaries between SCoNP and the ecological corridor where fires of almost the same shape took place in 2010 and in 2015.

## 4. Conclusions

In this article, we presented a fire scar database of burned areas for the first time in the Capivara-Confusões Mosaic, located in a Caatinga-Cerrado ecotone. This study contributes to the establishment that fire is a main concern in these protected areas. Fire regimes were found to be very different between SCanP, SCoNP, the ecological corridor and the surroundings; thus, to design proper management policies to prevent fire or to implement an IFM, the specific temporal and spatial pattern needs to be considered.

We analyzed yearly, seasonal and monthly amounts of burned area, its spatial distribution and recurrence dynamics and discussed the relations between precipitation, productivity, biomass moisture, proximity to roads and settlements, and protected area efficiency.

The integration of satellite imagery with ground-based precipitation data allowed a long-term, fine-spatial resolution and landscape-scale approach. Landsat long-time series availability was used to cover a 19-

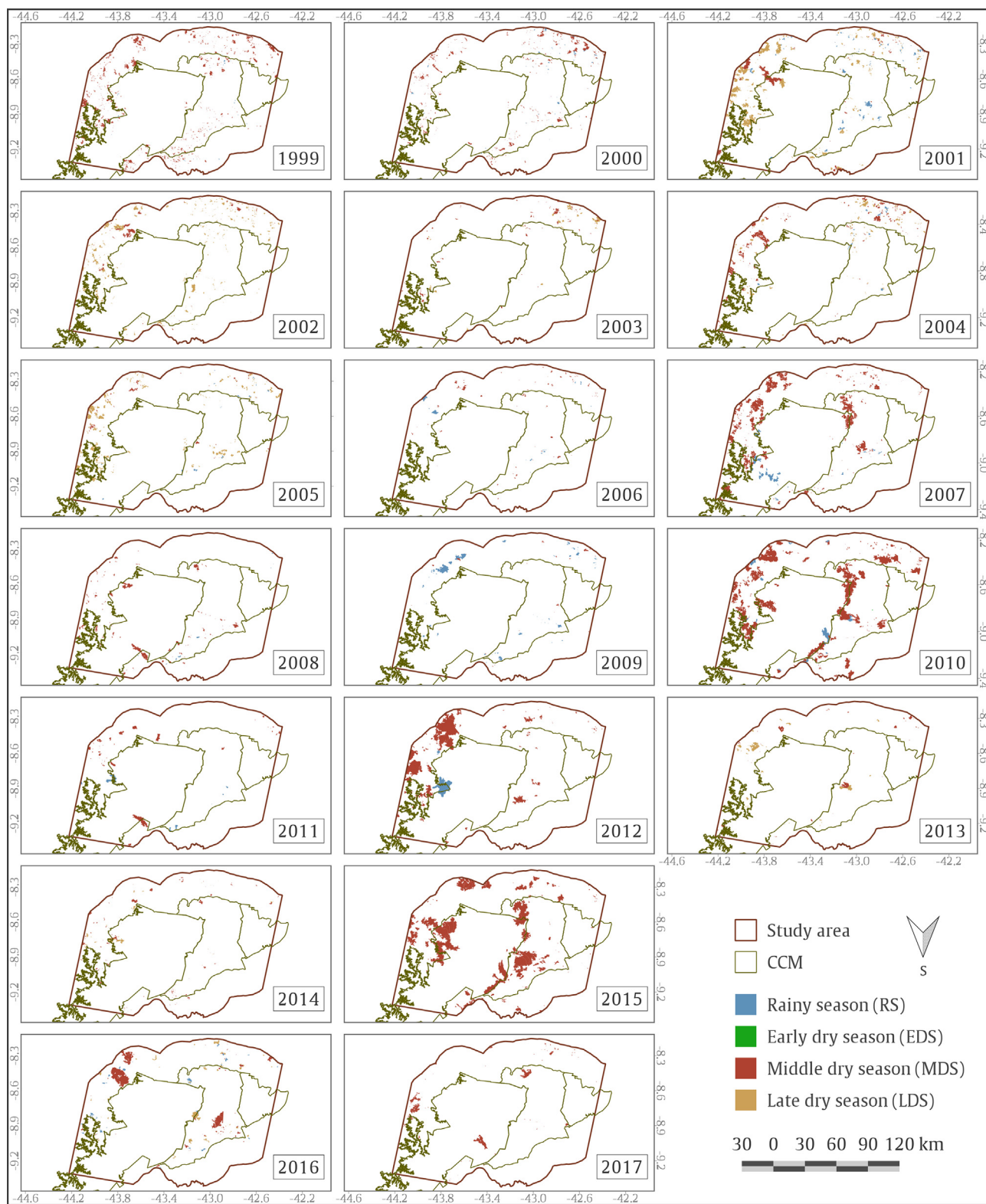


**Fig. 6.** Mapping of the yearly and seasonal distribution of fire scars inside the study area from 1999 to 2017 of the Capivara-Confusões Mosaic (CCM). Areas not colored represent unburned areas during the respective year.

year long study, and its 30 m resolution supported the identification of small burned patches. The use of daily precipitation data from local meteorological stations allowed a dynamic approach to yearly burning seasons, avoiding the error associated with a static definition of these periods, which is important because the region presents high inter-annual variations in precipitation. The subdivision of the dry season

seems to appropriately capture the different moisture conditions that drive fire activity, with most burned areas in the driest season and with the late transition stage burning more than the early.

The burned area database generated here, and the fire regime description, might assist studies of postfire Caatinga vegetation dynamics that until now have been poorly explored, such as the analysis of

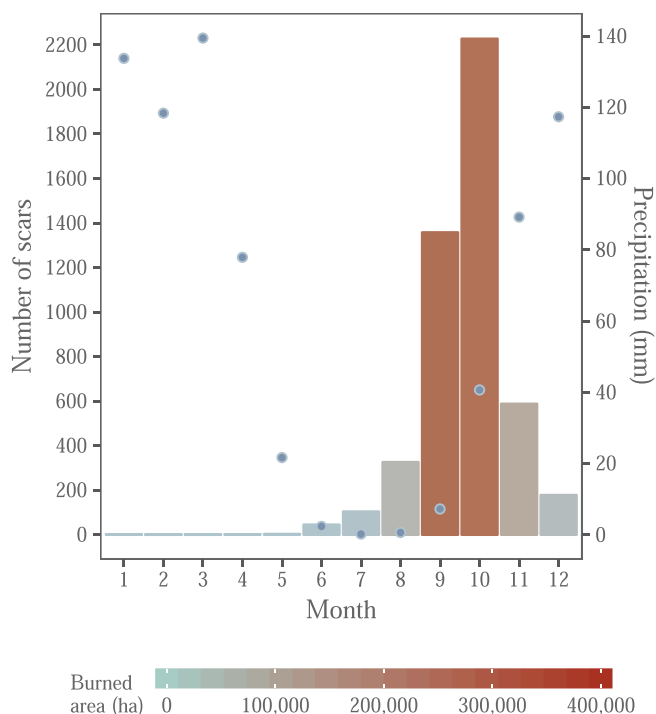


**Fig. 7.** Number of scars and amount of burned area by month, together with mean monthly precipitation over the period 1999 to 2017 in the Capivara-Confusões Mosaic and its surroundings. Blue dots represent the mean monthly precipitation between 1984 and 2018, bars represent the number of scars, and the colored gradient represents the amount of burned area.

vegetation response to fire and fire recurrence, regeneration strategies or the effects of fire on vegetation structure and floristic biodiversity. Finally, the mapping of fire recurrence and the identification of areas with moderate recurrence might help in the construction of fire risk maps for the two protected areas and their surroundings. This is particularly important for the region, not only because the Capivara-Confusões Mosaic is the largest conservation area of Caatinga vegetation but also to help protect numerous archaeological sites that might be at risk of losing historical evidence because of fires.

**CRedit authorship contribution statement**

**Daihana S. Argibay:** Conceptualization, Methodology, Formal analysis, Investigation, Writing - original draft, Visualization. **Javier Sparacino:** Methodology, Investigation, Writing - review & editing, Visualization. **Giovana M. Espindola:** Conceptualization, Writing - review & editing, Supervision, Project administration, Funding acquisition.

**Declaration of Competing Interest**

The authors declare that they have no known competing financial interests or personal relationships that could have appeared to influence the work reported in this paper.

**Acknowledgments**

This study was carried out within the project “Diagnosis of forest fires occurrence in the Serra das Confusões and Serra da Capivara National Parks, Piauí, Brazil”, funded by the National Council for Scientific and Technological Development – CNPq, [grant number Proc 421178/2017-5]. We thank ICMBio (Instituto Chico Mendes de

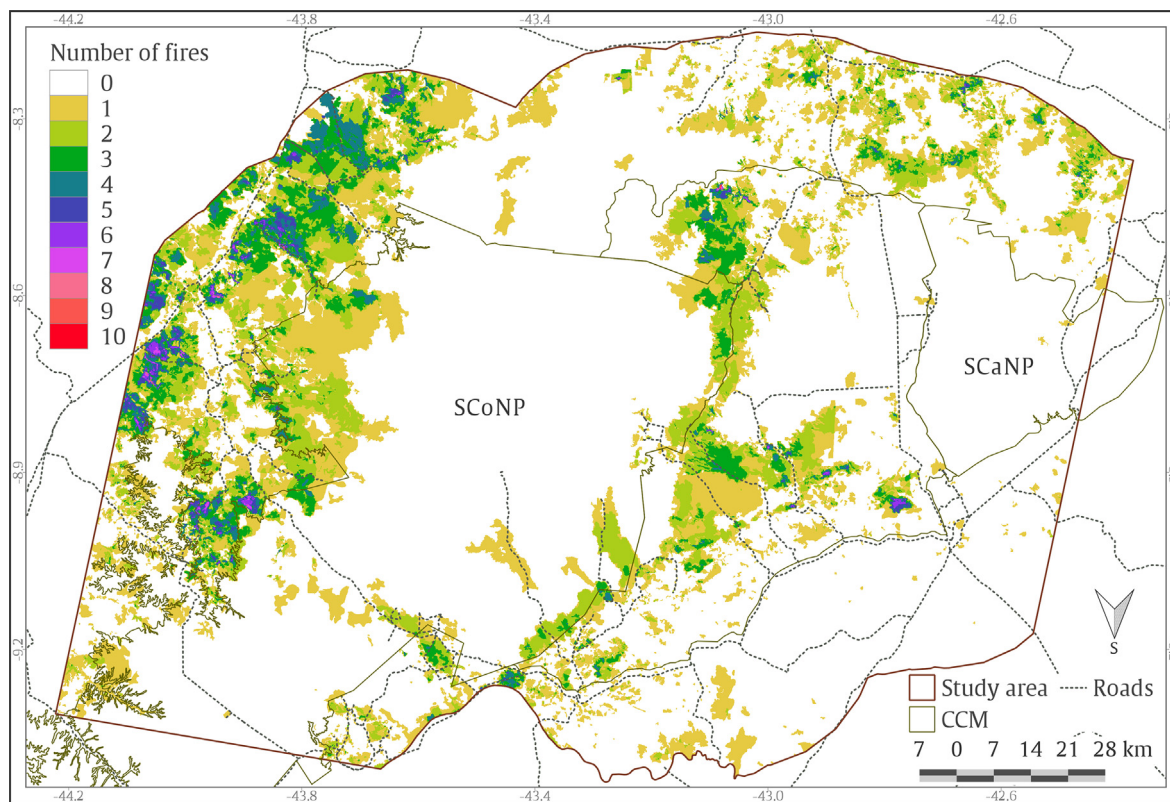


**Fig. 8.** Mapping of fire recurrence from 1999 to 2017 in the Capivara-Confusões Mosaic and its surroundings. The palette of colors represents the number of times that the same area burned. White areas were never burned during this period. Landsat 5 TM, Landsat 7 ETM+ and Landsat 8 OLI images were used for the delimitation of burned areas. Spatial resolution is 30 m.

Conservação da Biodiversidade) for the research license and the FUMDHAM (Fundação Museu do Homem Americano) for providing digital material. DSA received a master's scholarship from PAEC/GCUB/OAS. JS received a fellowship from CNPq. We would also like to thank the reviewers for their thoughtful comments and efforts towards improving our manuscript.

## Declaration of interests

None

## Appendix A. Supplementary data

Supplementary data to this article can be found online at <https://doi.org/10.1016/j.ecolind.2020.106151>.

## References

- Alvarado, S.T., Fornazari, T., Cóstola, A., Morellato, L.P.C., Silva, T.S.F., 2017. Drivers of fire occurrence in a mountainous Brazilian cerrado savanna: tracking long-term fire regimes using remote sensing. *Ecol. Indic.* 78, 270–281. <https://doi.org/10.1016/j.ecolind.2017.02.037>.
- Alvarado, S.T., Andela, N., Silva, T.S.F., Archibald, S., 2019. Thresholds of fire response to moisture and fuel load differ between tropical savannas and grasslands across continents. *Global Ecol. Biogeogr.* 00, 1–14. <https://doi.org/10.1111/geb.13034>.
- Alves, D.B., Pérez-Cabello, F., 2017. Multiple remote sensing data sources to assess spatio-temporal patterns of fire incidence over Campos Amazônicos Savanna Vegetation Enclave (Brazilian Amazon). *Sci. Total Environ.* 601–602, 142–158. <https://doi.org/10.1016/j.scitotenv.2017.05.194>.
- ANA-Agencia Nacional das Águas, 2017. Available online: <http://snirh.gov.br/> (accessed on 13 September 2017).
- Aragão, L.E., Anderson, L.O., Fonseca, M.G., Rosan, T.M., Vedovato, L.B., Wagner, F.H., Silva, C.V.J., Silva, C.H.L., Arai, E., Aguiar, A.P., Barlow, J., Berenguer, E., Deeter, M.N., Domingues, L.G., Gatti, L., Gloor, M., Malhi, Y., Marengo, J.A., Miller, J.B., Phillips, O.L., Saatchi, S., 2018. 21st Century drought-related fires counteract the decline of Amazon deforestation carbon emissions. *Nat. Commun.* 9 (1), 536. <https://doi.org/10.1038/s41467-017-02771-y>.
- Archibald, S., Lehmann, C.E.R., Belcher, C.M., Bond, W.J., Bradstock, R.A., Daniau, A.-L., Dexter, K.G., Forrester, E.J., Greve, M., He, T., Higgins, S.I., Hoffmann, W.A., Lamont, B.B., McGlenn, D.J., Moncrieff, G.R., Osborne, C.P., Pausas, J.G., Price, O., Ripley, B.S., Rogers, B.M., Schwill, D.W., Simon, M.F., Turetsky, M.R., Van der Werf, G.R., Zanne, A.E., 2018. Biological and geophysical feedbacks with fire in the Earth system. *Environ. Res. Lett.* 13, 033003. <https://doi.org/10.1088/1748-9326/aa9ead>.
- Archibald, S., Lehmann, C.E.R., Gomez-Dans, J.L., Bradstock, R.A., 2013. Defining pyromes and global syndromes of fire regimes. *Proc. Natl. Acad. Sci.* 110, 6442–6447. <https://doi.org/10.1073/pnas.1211466110>.
- Archibald, S., Roy, D.P., van Wilgen, B.W., Scholes, R.J., 2009. What limits fire? An examination of drivers of burnt area in Southern Africa. *Glob. Change Biol.* 15, 613–630. <https://doi.org/10.1111/j.1365-2486.2008.01754.x>.
- Argañaraz, J.P., Landi, M.A., Scavuzzo, C.M., Bellis, L.M., 2018. Determining fuel moisture thresholds to assess wildfire hazard: A contribution to an operational early warning system. *PLoS ONE* 13 (10), e0204889. <https://doi.org/10.1371/journal.pone.0204889>.
- Argañaraz, J.P., Pizarro, G.G., Zak, M., Bellis, L.M., 2015. Fire regime, climate, and vegetation in the Sierras de Córdoba, Argentina. *Fire Ecol.* 11, 55–73. <https://doi.org/10.4996/fireecology.1101055>.
- Barbosa, H.A., Lakshmi Kumar, T.V., Paredes, F., Elliott, S., Ayuga, J.G., 2019. Assessment of Caatinga response to drought using Meteosat-SEVIRI Normalized Difference Vegetation Index (2008–2016). *ISPRS J. Photogramm. Remote Sens.* 148, 235–252. <https://doi.org/10.1016/j.isprsjprs.2018.12.014>.
- Bastarrrika, A., Alvarado, M., Artano, K., Martínez, M., Mesanza, A., Torre, L., Ramo, R., Chuvieco, E., 2014. BAMS: a tool for supervised burned area mapping using landsat data. *Remote Sens.* 6, 12360–12380. <https://doi.org/10.3390/rs61212360>.
- Bastarrrika, A., Chuvieco, E., Martín, M.P., 2011. Mapping burned areas from Landsat TM/ETM+ data with a two-phase algorithm: Balancing omission and commission errors. *Remote Sens. Environ.* 115, 1003–1012. <https://doi.org/10.1016/j.rse.2010.12.005>.
- Batista, E.K.L., Russell-Smith, J., França, H., Figueira, J.E.C., 2018. An evaluation of contemporary savanna fire regimes in the Canastra National Park, Brazil: Outcomes of fire suppression policies. *J. Environ. Manag.* 205, 40–49. <https://doi.org/10.1016/j.jenvman.2017.09.053>.
- Bivand, R., Keitt, T., Rowlingson, B., Pebesma, E., Sumner, M., & Hijmans, R., 2015. rgdal: Bindings for the Geospatial Data Abstraction Library 2017. R package version 0.8-13.
- Bond, W., Keeley, J., 2005. Fire as a global 'herbivore': the ecology and evolution of flammable ecosystems. *Trends Ecol. Evol.* 20, 387–394. <https://doi.org/10.1016/j.tree.2005.04.025>.
- Bond, W.J., Woodward, F.I., Midgley, G.F., 2004. The global distribution of ecosystems in a world without fire. *New Phytol.* 165, 525–538. <https://doi.org/10.1111/j.1469-8137.2004.01252.x>.
- Bowman, D.M., Balch, J.K., Artaxo, P., Bond, W.J., Carlson, J.M., Cochrane, M.A., Johnston, F.H., 2009. Fire in the Earth system. *Science* 324 (5926), 481–484. <https://doi.org/10.1126/science.1163886>.
- Bowman, D.M.J.S., Balch, J., Artaxo, P., Bond, W.J., Cochrane, M.A., D'Antonio, C.M., DeFries, R., Johnston, F.H., Keeley, J.E., Krawchuk, M.A., Kull, C.A., Mack, M., Moritz, M.A., Pyne, S., Roos, C.I., Scott, A.C., Sodhi, N.S., Swetnam, T.W., 2011. The human dimension of fire regimes on Earth: The human dimension of fire regimes on Earth. *J. Biogeogr.* 38, 2223–2236. <https://doi.org/10.1111/j.1365-2699.2011.02595.x>.
- Bradstock, R.A., 2010. A biogeographic model of fire regimes in Australia: current and future implications. *Glob. Ecol. Biogeogr.* 19, 145–158. <https://doi.org/10.1111/j.1466-8238.2009.00512.x>.
- Cardozo, F., Pereira, G., Shimabukuro, Y., Moraes, E., 2014. Analysis and assessment of the spatial and temporal distribution of burned areas in the Amazon Forest. *Remote Sens.* 6, 8002–8025. <https://doi.org/10.3390/rs6098002>.
- Chen, Y., Morton, D.C., Andela, N., van der Werf, G.R., Giglio, L., Randerson, J.T., 2017. A pan-tropical cascade of fire driven by El Niño/Southern Oscillation. *Nat. Clim. Change* 7, 906–911. <https://doi.org/10.1038/s41558-017-0014-8>.
- Chuvieco, E., Yule, C., Heil, A., Mouillot, F., Alonso-Canas, I., Padilla, M., Pereira, J.M., Oom, D., Tansey, K., 2016. A new global burned area product for climate assessment of fire impacts. *Glob. Ecol. Biogeogr.* 25, 619–629. <https://doi.org/10.1111/geb.12440>.
- Claval, P., de Freitas, I.A., 2007. Seasonality in Brazil: rain, mud and drought. In: Palang, H., Sooväli, H., Printsmann, A. (Eds.), *Seasonal Landscapes*. Springer, Netherlands, Dordrecht, pp. 61–83. [https://doi.org/10.1007/1-4020-4990-0\\_3](https://doi.org/10.1007/1-4020-4990-0_3).
- Collevatti, R.G., Terribile, L.C., de Oliveira, G., Lima-Ribeiro, M.S., Nabout, J.C., Rangel, T.F., Diniz-Filho, J.A.F., 2013. Drawbacks to palaeodistribution modelling: the case of South American seasonally dry forests. *J. Biogeogr.* 40, 345–358. <https://doi.org/10.1111/jbi.12005>.
- Coutinho, L.M., 1982. Ecological effects of fire in Brazilian cerrado. In *Ecology of tropical savannas*. Springer, Berlin, Heidelberg, pp. 273–291. [https://doi.org/10.1007/978-3-642-68786-0\\_13](https://doi.org/10.1007/978-3-642-68786-0_13).
- Dai, A., 2011. Drought under global warming: a review. *WIREs Clim. Change* 2 (1), 45–65. <https://doi.org/10.1002/wcc.81>.
- Daldegan, G., de Carvalho, O., Guimarães, R., Gomes, R., Ribeiro, F., McManus, C., 2014. Spatial patterns of fire recurrence using remote sensing and GIS in the Brazilian Savanna: Serra do Tombador nature reserve. *Brazil. Remote Sens.* 6, 9873–9894. <https://doi.org/10.3390/rs6109873>.
- Durigan, G., Ratter, J.A., 2016. The need for a consistent fire policy for Cerrado conservation. *J. Appl. Ecol.* 53 (1), 11–15. <https://doi.org/10.1111/1365-2664.12559>.
- Eidenshink, J., Schwind, B., Brewer, K., Zhu, Z.-L., Quayle, B., Howard, S., 2007. A project for monitoring trends in burn severity. *Fire Ecol.* 3, 3–21. <https://doi.org/10.4996/fireecology.0301003>.
- Eiten, G., 1972. The cerrado vegetation of Brazil. *Bot. Rev.* 38, 201–341. <https://doi.org/10.1007/BF02859158>.
- Emperaire, L., 1989. *Végétation et gestion des ressources naturelles dans la Caatinga du Sud-Est du Piauí (Brésil)*. Doctorat d'Etat ès Sciences Naturelles, Université Pierre et Marie Curie. Paris, p. 378.
- Feeley, K.J., Gillespie, T.W., Terborgh, J.W., 2005. The Utility of spectral indices from Landsat ETM+ for measuring the structure and composition of tropical dry forests. *Biotropica* 37, 508–519. <https://doi.org/10.1111/j.1744-7429.2005.00069.x>.
- Field, C.B., 1998. Primary production of the biosphere: integrating terrestrial and oceanic components. *Science* 281, 237–240. <https://doi.org/10.1126/science.281.5374.237>.
- Flannigan, M.D., Krawchuk, M.A., de Groot, W.J., Wotton, B.M., Gowman, L.M., 2009. Implications of changing climate for global wildland fire. *Int. J. Wildland Fire* 18, 483. <https://doi.org/10.1071/WF08187>.
- Fontugne, M., Shao, Q., Frank, N., Thil, F., Guidon, N., Boeda, E., 2013. Cross-dating (Th/U-<sup>14</sup>C) of calcite covering prehistoric paintings at Serra da Capivara National Park, Piauí, Brazil. *Radiocarbon* 55 (3), 1191–1198. <https://doi.org/10.1017/S0033822200048104>.
- Hijmans, R., 2017. raster: geographic data analysis and modeling version 2.5–2. 2015. Hoffmann, W.A., Jaconis, S.Y., Mckinley, K.L., Geiger, E.L., Gotsch, S.G., Franco, A.C., 2012. Fuels or microclimate? Understanding the drivers of fire feedbacks at savanna-forest boundaries. *Austral Ecol.* 37, 634–643. <https://doi.org/10.1111/j.1442-9993.2011.02324.x>.
- IBGE-Instituto Brasileiro de Geografia e Estatística, 2017. Available online: <http://downloads.ibge.gov.br/> (accessed on 13 September 2017).
- ICNF-Institute for Nature Conservation and Forests of Portugal, 2018. Cartografia nacional de áreas ardidas. <http://www.icnf.pt/portal/florestas/dpci/inc/info-geo> (accessed 15 August 2018).
- Jarvis, A., Reuter, H.I., Nelson, A., Guevara, E., 2008. Hole-Filled Seamless SRTM Data V4. International Centre for Tropical Agriculture (CIAT): Palmira, Colombia.
- Kauffman, J.B., Sanford Jr, R.L., Cummings, D.L., Salcedo, I.H., Sampaio, E.V.S.B., 1993. Biomass and nutrient dynamics associated with slash fires in neotropical dry forests. *Ecology* 74 (1), 140–151. <https://doi.org/10.2307/1939509>.
- Keeley, J.E., 2009. Fire intensity, fire severity and burn severity: a brief review and suggested usage. *Int. J. Wildland Fire* 18 (1), 116–126. <https://doi.org/10.1071/WF07049>.
- Key, C.H., Benson, N.C., 2006. Landscape Assessment (LA) 55. FIREMON: Fire effects monitoring and inventory system. Gen. Tech. Rep. RMRS-GTR-164-CD, Fort Collins, CO: US Department of Agriculture, Forest Service, Rocky Mountain Research Station.
- Kousky, V.E., Chug, P.S., 1978. Fluctuations in annual rainfall for Northeast Brazil. *J. Meteorol. Soc. Jpn. Ser. II* 56 (5), 457–465. [https://doi.org/10.2151/jmsj1965.56\\_5\\_457](https://doi.org/10.2151/jmsj1965.56_5_457).
- Lahaye, C., Hernandez, M., Boeda, E., Felice, G.D., Guidon, N., Hoeltz, S., Lourdeau, A., Pagli, M., Pessis, A.M., Rasse, M., Viana, S., 2013. Human occupation in South America by 20,000 BC: the Toca da Tira Peia site, Piauí, Brazil. *J. Archaeol. Sci.* 40 (6), 2840–2847. <https://doi.org/10.1016/j.jas.2013.02.019>.

- Lehmann, C.E., Archibald, S.A., Hoffmann, W.A., Bond, W.J., 2011. Deciphering the distribution of the savanna biome. *New Phytol.* 191 (1), 197–209.
- Lemes, G.P., Matricardi, E.A.T., Costa, O.B., Leal, F.A., 2014. Spatiotemporal assessment of forest fires occurred in the Serra da Canastra National Park between 1991 and 2011. *Ambiência* 10. <https://doi.org/10.5935/ambiencia.2014.supl.03>.
- Lemos, J.R., Rodal, M.J.N., 2002. Fitossociologia do componente lenhoso de um trecho da vegetação de caatinga no Parque Nacional Serra da Capivara, Piauí, Brasil. *Acta Bot. Bras.* 16, 23–42. <https://doi.org/10.1590/S0102-33062002000100005>.
- Lentile, L.B., Holden, Z.A., Smith, A.M., Falkowski, M.J., Hudak, A.T., Morgan, P., Lewis, S.A., Gessler, P.E., Benson, N.C., 2006. Remote sensing techniques to assess active fire characteristics and post-fire effects. *Int. J. Wildland Fire* 15 (3), 319–345. <https://doi.org/10.1071/WF05097>.
- Libonati, R., Camara, C.C. da, Setzer, A.W., Morelli, F., Jesus, S.C. de, Candido, P.A., Melchiori, A.E., 2014. Validation of the burned area “(V,W)” Modis algorithm in Brazil, in: *Advances in Forest Fire Research*. Imprensa da Universidade de Coimbra, pp. 1774–1785. [https://doi.org/10.14195/978-989-26-0884-6\\_197](https://doi.org/10.14195/978-989-26-0884-6_197).
- Libonati, R., DaCamara, C., Setzer, A., Morelli, F., Melchiori, A., 2015. An algorithm for burned area detection in the Brazilian cerrado using 4 µm MODIS imagery. *Remote Sens.* 7, 15782–15803. <https://doi.org/10.3390/rs71115782>.
- Liebmann, B., Camargo, S.J., Seth, A., Marengo, J.A., Carvalho, L.M.V., Allured, D., Fu, R., Vera, C.S., 2007. Onset and end of the rainy season in South America in observations and the ECHAM 4.5 atmospheric general circulation model. *J. Clim.* 20 (10), 2037–2050. <https://doi.org/10.1175/JCLI4122.1>.
- Liu, W.T., Juárez, R.I.N., 2001. ENSO drought onset prediction in northeast Brazil using NDVI. *Int. J. Remote Sens.* 22, 3483–3501. <https://doi.org/10.1080/01431160010006430>.
- Liu, H., Park Williams, A., Allen, C.D., Guo, D., Wu, X., Anenkhonov, O.A., Liang, E., Sandanov, D.V., Yin, Y., Zhaohuan, Q., Badmaeva, N.K., 2013. Rapid warming accelerates tree growth decline in semi-arid forests of Inner Asia. *Glob. Change Biol.* 19 (8), 2500–2510. <https://doi.org/10.1111/gcb.12217>.
- Marengo, J.A., Torres, R.R., Alves, L.M., 2017. Drought in Northeast Brazil—past, present, and future. *Theor. Appl. Climatol.* 129, 1189–1200. <https://doi.org/10.1007/s00704-016-1840-8>.
- Martínez-Ramos, M., Balvanera, P., Arreola Villa, F., Mora, F., Maass, J.M., Maza-Villalobos Méndez, S., 2018. Effects of long-term inter-annual rainfall variation on the dynamics of regenerative communities during the old-field succession of a neotropical dry forest. *For. Ecol. Manage.* 426, 91–100. <https://doi.org/10.1016/j.foreco.2018.04.048>.
- Masek, J.G., Vermote, E.F., Saleous, N.E., Wolfe, R., Hall, F.G., Huemmrich, K.F., Lim, T.K., 2006. A Landsat surface reflectance dataset for North America, 1990–2000. *IEEE Geosci. Remote Sens. Lett.* 3 (1), 68–72. <https://doi.org/10.1109/LGRS.2005.857030>.
- Mayr, M.J., Vanselow, K.A., Samimi, C., 2018. Fire regimes at the arid fringe: A 16-year remote sensing perspective (2000–2016) on the controls of fire activity in Namibia from spatial predictive models. *Ecol. Indic.* 91, 324–337. <https://doi.org/10.1016/j.ecolind.2018.04.022>.
- Melchiori, A.E., W. Setzer, A., Morelli, F., Libonati, R., Cândido, P. de A., Jesús, S.C. de, 2014. A Landsat-TM/OLI algorithm for burned areas in the Brazilian Cerrado: preliminary results, in: *Advances in Forest Fire Research*. Imprensa da Universidade de Coimbra, pp. 1302–1311. [https://doi.org/10.14195/978-989-26-0884-6\\_143](https://doi.org/10.14195/978-989-26-0884-6_143).
- Meng, R., Zhao, F., 2017. Remote sensing of fire effects: A review for recent advances in burned area and burn severity mapping. In: *Remote Sensing of Hydrometeorological Hazards*. [s.l.] Petropolis, G. P.; ISLAM, T., p. 261–281.
- Miranda, H.S., Sato, M.N., Neto, W.N., Aires, F.S., 2009. Fires in the cerrado, the Brazilian savanna, in: *Tropical fire ecology*. Springer, Berlin, Heidelberg, pp. 427–450. [https://doi.org/10.1007/978-3-540-77381-8\\_15](https://doi.org/10.1007/978-3-540-77381-8_15).
- MMA-Ministério do Meio Ambiente, 2017. Available online: <http://mma.gov.br/> (accessed on 13 September 2017).
- Moreno, M.V., Conedera, M., Chuvieco, E., Pezzatti, G.B., 2014. Fire regime changes and major driving forces in Spain from 1968 to 2010. *Environ. Sci. Policy* 37, 11–22. <https://doi.org/10.1016/j.envsci.2013.08.005>.
- Morgan, P., Hardy, C.C., Swetnam, T.W., Rollins, M.G., Long, D.G., 2001. Mapping fire regimes across time and space: Understanding coarse and fine-scale fire patterns. *Int. J. Wildland Fire* 10, 329. <https://doi.org/10.1071/WF01032>.
- Mouillot, F., Schultz, M.G., Yue, C., Cadule, P., Tansey, K., Ciaís, P., Chuvieco, E., 2014. Ten years of global burned area products from spaceborne remote sensing—A review: Analysis of user needs and recommendations for future developments. *Int. J. Appl. Earth Obs. Geoinformation* 26, 64–79. <https://doi.org/10.1016/j.jag.2013.05.014>.
- Moura, A.C.D.A., 2005a. Capuchin Monkey and the Caatinga Dry Forest: A Hard Life in a Harsh Habitat (Doctoral dissertation). University of Cambridge.
- Moura, L.S., 2005b. Estudo da Paisagem da Caatinga Piauiense: Parque Nacional Serra das Confusões-PI. Geografia (Master dissertation, UFPI). Teresina-PI 9, 1–26.
- Murphy, B.P., Bradstock, R.A., Boer, M.M., Carter, J., Cary, G.J., Cochrane, M.A., Fensham, R.J., Russell-Smith, J., Williamson, G.J., Bowman, D.M.J.S., 2013. Fire regimes of Australia: a pyrogeographic model system. *J. Biogeogr.* 40, 1048–1058. <https://doi.org/10.1111/jbi.12065>.
- Nogueira, J., Rambal, S., Barbosa, J., Mouillot, F., 2017a. Spatial pattern of the seasonal drought/burned area relationship across Brazilian biomes: sensitivity to drought metrics and global remote-sensing fire products. *Climate* 5, 42. <https://doi.org/10.3390/cli5020042>.
- Nogueira, J., Ruffault, J., Chuvieco, E., Mouillot, F., 2017b. Can we go beyond burned area in the assessment of global remote sensing products with fire patch metrics? *Remote Sens.* 9, 7. <https://doi.org/10.3390/rs9010007>.
- Oliveira, A.P.C., Bernard, E., 2017. The financial needs vs. the realities of in situ conservation: an analysis of federal funding for protected areas in Brazil's Caatinga. *Biotropica* 49, 745–752. <https://doi.org/10.1111/btp.12456>.
- Olmos, F., Albano, C., 2012. As aves da região do Parque Nacional Serra da Capivara (Piauí, Brasil). *Rev. Bras. Ornit.* 20 (3), 173–187.
- Olmos, F., 1992. Serra Da Capivara National Park and the conservation of north-eastern Brazil's caatinga. *Oryx* 26, 142. <https://doi.org/10.1017/S0030605300023565>.
- Pivello, V.R., 2011. The use of fire in the cerrado and amazonian rainforests of Brazil: past and present. *Fire Ecol.* 7, 24. <https://doi.org/10.4996/fireecology.0701024>.
- Pourtaghi, Z.S., Pourghasemi, H.R., Aretano, R., Semeraro, T., 2016. Investigation of general indicators influencing on forest fire and its susceptibility modeling using different data mining techniques. *Ecol. Indic.* 64, 72–84. <https://doi.org/10.1016/j.ecolind.2015.12.030>.
- Prado, D., 2003. As caatingas da América do Sul, in: I.R. Leal, M. Tabarelli, J.M.C. Silva (eds.). *Ecologia e conservação da Caatinga*. Editora Universitária, Universidade Federal de Pernambuco, Recife, Brasil, pp. 3–73.
- QGIS Development Team, 2018. Quantum GIS Geographic Information System. Open Source. Geospatial Foundation Project.
- R Core Team, 2017. R: a language and environment for statistical computing (version 3.4.2). R Foundation for Statistical Computing, Vienna, Austria.
- Ramos, R.P.L., 1975. Precipitation characteristics in the Northeast Brazil dry region. *J. Geophys. Res.* 80, 1665–1678. <https://doi.org/10.1029/JC080i012p01665>.
- Ramos-Neto, M.B., Pivello, V.R., 2000. Lightning fires in a Brazilian savanna national park: rethinking management strategies. *Environ. Manage.* 26, 675. <https://doi.org/10.1007/s002670010124>.
- Reddy, S.J., 1983. Climatic classification: the semi-arid tropics and its environment a review. *Embrapa Semiárido. Pesqui. Agropec. Bras.* 18 (8), 823–847.
- Rodrigues, R.R., McPhaden, M.J., 2014. Why did the 2011–2012 La Niña cause a severe drought in the Brazilian Northeast? *Geophys. Res. Lett.* 41 (3), 1012–1018. <https://doi.org/10.1002/2013GL058703>.
- Sampaio, E.V.S.B., Salcedo, I.H., Kauffman, J.B., 1993. Effect of Different Fire Severities on Coppicing of Caatinga Vegetation in Serra Talhada, PE, Brazil. *Biotropica* 25, 452. <https://doi.org/10.2307/2388868>.
- Sampaio, E.V.S.B., de Lima Araújo, E., Salcedo, I.H., Tiessen, H., 1998. Regeneração da vegetação de caatinga após corte e queima, em Serra Talhada. PE. *Pesqui. Agropec. Bras.* 33 (5), 621–632.
- Sampaio, E.V.S.B., Araújo, M.S.B., Sampaio, Y.S.B., 2005. Impactos ambientais da agricultura no processo de desertificação no Nordeste do Brasil. *Revista de Geografia, Recife* 22 (1), 90–112.
- Sano, E.E., Ferreira, L.G., Asner, G.P., Steinke, E.T., 2007. Spatial and temporal probabilities of obtaining cloud-free Landsat images over the Brazilian tropical savanna. *Int. J. Remote Sens.* 28, 2739–2752. <https://doi.org/10.1080/01431160600981517>.
- Schmidt, I.B., Moura, L.C., Ferreira, M.C., Eloy, L., Sampaio, A.B., Dias, P.A., Berlink, C.N., 2018. Fire management in the Brazilian savanna: first steps and the way forward. *J. Appl. Ecol.* 55 (5), 2094–2101. <https://doi.org/10.1111/1365-2664.13118>.
- Scott, A., 2000. The Pre-Quaternary history of fire. *Palaeogeogr. Palaeoclimatol. Palaeoecol.* 164, 281–329. [https://doi.org/10.1016/S0031-0182\(00\)00192-9](https://doi.org/10.1016/S0031-0182(00)00192-9).
- Silveira, L., Jácomo, A.T.A., Astete, S., Sollmann, R., Tórres, N.M., Furtado, M.M., Marinho-Filho, J., 2010. Density of the Near Threatened jaguar *Panthera onca* in the caatinga of north-eastern Brazil. *Oryx* 44, 104. <https://doi.org/10.1017/S0030605309990433>.
- Sparacino, J., Argibay, D. S., Espindola, G., 2019. Long-term (35 years) rainy and dry season characterization in semi-arid northeastern Brazil. Unpublished manuscript.
- U.S.G.S., 2018. Landsat collections: U.S. Geological Survey Fact Sheet 2018–3049, p. 2. <https://doi.org/10.3133/fs20183049>.
- U.S.G.S., 2006. EROS Archive, Digital Elevation, Shuttle Radar Topography Mission (SRTM) 1 Arc-Second Global. <http://doi.org/10.5066/F7PR7FTT>.
- Van Der Werf, G.R., Randerson, J.T., Giglio, L., Gobron, N., Dolman, A.J., 2008. Climate controls on the variability of fires in the tropics and subtropics. *Global Biogeochem. Cycles* 22 (3), GB3028. <https://doi.org/10.1029/2007GB003122>.
- Vermote, E., Justice, C., Claverie, M., Franch, B., 2016. Preliminary analysis of the performance of the Landsat 8/OLI land surface reflectance product. *Remote Sens. Environ.* 185, 46–56. <https://doi.org/10.1016/j.rse.2016.04.008>.